



Delft University of Technology

Efficient Massive Machine Type Communication (mMTC) via AMP

Mohammadkarimi, Mostafa; Ardkani, Masoud

DOI

[10.1109/LWC.2023.3256300](https://doi.org/10.1109/LWC.2023.3256300)

Publication date

2023

Document Version

Final published version

Published in

IEEE Wireless Communications Letters

Citation (APA)

Mohammadkarimi, M., & Ardkani, M. (2023). Efficient Massive Machine Type Communication (mMTC) via AMP. *IEEE Wireless Communications Letters*, 12(6), 1002-1006.

<https://doi.org/10.1109/LWC.2023.3256300>

Important note

To cite this publication, please use the final published version (if applicable).

Please check the document version above.

Copyright

Other than for strictly personal use, it is not permitted to download, forward or distribute the text or part of it, without the consent of the author(s) and/or copyright holder(s), unless the work is under an open content license such as Creative Commons.

Takedown policy

Please contact us and provide details if you believe this document breaches copyrights.

We will remove access to the work immediately and investigate your claim.

Green Open Access added to TU Delft Institutional Repository

'You share, we take care!' - Taverne project

<https://www.openaccess.nl/en/you-share-we-take-care>

Otherwise as indicated in the copyright section: the publisher is the copyright holder of this work and the author uses the Dutch legislation to make this work public.

Efficient Massive Machine Type Communication (mMTC) via AMP

Mostafa Mohammadkarimi[✉], Member, IEEE, and Masoud Ardakani[✉], Senior Member, IEEE

Abstract—We propose efficient and low-complexity multiuser detection (MUD) algorithms for Gaussian multiple access channel (G-MAC) for short-packet transmission in massive machine type communications. To do so, we first formulate the G-MAC MUD problem as a sparse signal recovery problem and obtain the exact and approximate joint prior distribution of the sparse vector to be recovered. Then, we employ the Bayesian approximate message passing (AMP) algorithms with the optimal separable and non-separable minimum mean squared error (MMSE) denoisers for soft decoding of the sparse vector. The effectiveness of the proposed MUD algorithms for a large number of devices is supported by simulation results. For packets of 8 information bits, while the state-of-the-art AMP with soft-threshold denoising achieves 8/100 of the upper bound at $E_b/N_0 = 4$ dB, the proposed algorithms reach 4/7 and 1/2 of the upper bound.

Index Terms—Multiuser detection, approximate message passing, IoT, Bayesian MMSE denoiser, sparse recovery, short packet.

I. INTRODUCTION

IN MANY Internet of Things (IoT) applications, massive machine-type communications (mMTC) services are required, where a large number of devices transmit very short packets to a base station (BS). Typically, these short packets are transmitted whenever a measured value changes; thus, sporadic traffic pattern is popular in mMTC [1], [2], [3]. Sparse signal processing for massive connectivity including data and activity detection has been studied in [3], [4], [5].

Recently, bounds on the exact block error probability of Gaussian random codes in additive white Gaussian noise (AWGN) for massive uplink multiple access (MA) at finite message length have been derived [6]. The author in [6] has shown that a promising solution to support massive uplink connectivity for short packet transmission is the Gaussian multiple access channel (G-MAC). The challenging task in the realization of G-MAC is the design of efficient and low-complexity multiuser detection (MUD) algorithms at the BS [7]. In [8], the iterative soft interference cancellation (SIC) decoding has been employed for the G-MAC with short packet transmission, but it suffers from error propagation.

In this letter, we propose two efficient and low-complexity MUD algorithms for the G-MAC for short-packet mMTC. We first formulate the MUD problem as an under-determined

Manuscript received 10 February 2023; accepted 1 March 2023. Date of publication 13 March 2023; date of current version 9 June 2023. This work was supported by the Natural Sciences and Engineering Research Council of Canada (NSERC). The associate editor coordinating the review of this article and approving it for publication was R. Wang. (*Corresponding author: Mostafa Mohammadkarimi*)

Mostafa Mohammadkarimi is with the Department of Microelectronics, Delft University of Technology, 2628 CD Delft, The Netherlands (e-mail: m.mohammadkarimi@tudelft.nl).

Masoud Ardakani is with the Department of Electrical and Computer Engineering, University of Alberta, Edmonton, AB T6G 2R3, Canada (e-mail: ardakani@ualberta.ca).

Digital Object Identifier 10.1109/LWC.2023.3256300

sparse signal recovery problem. Then, we propose to employ approximate message passing (AMP) for soft decoding of the short packets transmitted by the IoT devices in the network. In most MUD problems using AMP for soft decoding, the joint prior distribution of the vector to be recovered is generally assumed to be unknown. In such cases, the optimal minimum mean squared error (MMSE) denoiser cannot be employed, and thus; the denoiser is designed under the minimax framework to optimize the AMP algorithm performance for the worst-case or least-favorable distribution, leading to a soft-thresholding denoiser. However, in the problem at hand, the key idea is that we can obtain the exact and approximate prior joint distribution of the sparse vector to be recovered. Thus, the optimal separable and non-separable MMSE denoisers can be employed for Bayesian AMP soft decoding. The decoupling effect results in low-complexity MMSE denoising in each AMP iteration [9], [10], [11]. The contributions of this letter are:

- We formulate the problem of G-MAC MUD as a sparse signal recovery problem and obtain the exact and approximate prior joint distribution of the sparse vector to be recovered. The approximate prior distribution is obtained by minimizing the Kullback-Leibler divergence (KLD) as a measure of difference between probability densities.
- By taking into account the exact and the KLD-based approximate prior distribution of the sparse vector, we introduce two MUD algorithms called (i) the relaxed block sparsity AMP (RBS-AMP), and (ii) the block sparsity AMP (BS-AMP) MUD algorithms for G-MAC suitable for short packet transmission in mMTC.
- The multiuser efficiency (MUE) of the proposed MUD algorithms is derived and shown to be close to one.
- We show that our BS-AMP MUD algorithm results in a new achievability bound that is closer to the upper bound in [6] compared to the achievability bound of the RBS-AMP, the state of the art AMP soft decoding in [12], and the SIC decoding in [8].

Notation: The symbols $(\cdot)^T$, $\text{Tr}(\cdot)$, $\|\cdot\|_0$, and $\|\cdot\|$ show the transpose operator, trace of a matrix, 0-norm, and Euclidean norm of a vector, respectively. The symbol $\hat{\mathbf{x}}$ is an estimate of vector \mathbf{x} , and $\delta(\cdot)$ is the Dirac delta function.

II. SYSTEM MODEL

We consider an IoT network equipped with open loop power control (OLPC), where D IoT devices simultaneously communicate with a single BS. In the OPLC, there is dedicated pilot channel provided for channel estimation. Pilot signal is transmitted by the BS to all IoT devices in the network, and the IoT devices receive the pilot signal and estimate the power strength. Based on this estimate, each IoT device adjusts its transmit power accordingly to compensate the effect of channel [8]. In the uplink channel, each IoT device transmits K bits of information by using Gaussian random coding with codewords of length $M = nD$. The aggregate rate of the multiuser coded system is DK/M . For short packet transmission, the

received vector at the BS in vector form is

$$\mathbf{y} = \mathbf{Cx} + \mathbf{w}, \quad (1)$$

where $\mathbf{C} \in \mathbb{R}^{M \times N}$ has independent and identically distributed (i.i.d.) entries, $C_{ij} \sim \mathcal{N}(0, 1/M)$, $N \triangleq 2^K D$, and \mathbf{x} is a block sparse vector of length $N \times 1$ with the sparsity level D as

$$\mathbf{x} = [x_1 \ x_2 \ \dots \ x_N]^T = [\mathbf{x}_1^T \ \mathbf{x}_2^T \ \dots \ \mathbf{x}_D^T]^T, \quad (2)$$

where \mathbf{x}_q is a $2^K \times 1$ vector as $\|\mathbf{x}_q\|_0 = 1$, $q = 1, 2, \dots, D$. The $M \times 1$ vector \mathbf{w} in (1) is the AWGN vector with covariance matrix $\sigma_w^2 \mathbf{I}$. We assume that $\beta \triangleq \lim_{D \rightarrow \infty} M/N = n/(2^K) > 0$.

Because of the OLPC, the received power of the D IoT devices at the BS is fixed and is denoted by P_1 . In this case, the joint prior distribution of the transmit vector $\mathbf{x}_q \triangleq [x_{q,1}, x_{q,2}, \dots, x_{q,2^K}]^T$, $q = 1, 2, \dots, D$, in (2) is given by¹

$$f_{\mathbf{X}}(\mathbf{x}_q; P_1, K) = \sum_{k=1}^{2^K} \frac{1}{2^K} \delta(\mathbf{x}_q - \sqrt{P_1} \mathbf{e}_k), \quad (3)$$

where $\mathbf{e}_1, \mathbf{e}_2, \dots, \mathbf{e}_{2^K}$ are orthonormal basis in right-handed Cartesian coordinate system. Our goal is to design MUD algorithms to detect the K information bits transmitted by each IoT device. As \mathbf{x} is a block-sparse vector, we have a sparse signal reconstruction problem. In this letter, we adopt the low-complexity Bayesian AMP algorithms for signal recovery.

III. REVIEW OF AMP

In this section, we first briefly review AMP and its state evolution (SE) for the separable denoiser.

A. AMP Algorithm With Separable Denoiser

For noisy linear measurements of the form

$$\mathbf{s} = \mathbf{Au} + \mathbf{w}, \quad (4)$$

where $\mathbf{A} \in \mathbb{R}^{M \times N}$, $\mathbf{s} \in \mathbb{R}^{M \times 1}$, $\mathbf{u} \in \mathbb{R}^{N \times 1}$, and $\mathbf{w} \in \mathbb{R}^{M \times 1}$. AMP algorithm with denoiser $\eta_t : \mathbb{R}^N \rightarrow \mathbb{R}^N$ at the $(t+1)$ th iteration estimates vector \mathbf{u} as follows [13]

$$\hat{\mathbf{u}}^{t+1} = \eta_t(\mathbf{v}^t) = \eta_t(\hat{\mathbf{u}}^t + \mathbf{A}^T \mathbf{r}^t), \quad (5a)$$

$$\mathbf{r}^t = \mathbf{s} - \mathbf{A}\hat{\mathbf{u}}^t + \frac{N}{M} \mathbf{r}^{t-1} \text{div}(\eta_{t-1}(\mathbf{v}^{t-1})), \quad (5b)$$

$$\mathbf{v}^t = \hat{\mathbf{u}}^t + \mathbf{A}^T \mathbf{r}^t, \quad (5c)$$

where $\text{div}(\eta_t(\mathbf{g})) \triangleq \frac{1}{N} \text{Tr}(\frac{\partial \eta_t(\mathbf{g})}{\partial \mathbf{g}})$ with $\mathbf{g} \triangleq [g_1 \ g_2 \ \dots \ g_N]^T$, $\hat{\mathbf{u}}^0 = \mathbf{0}$, and $\mathbf{r}^0 = \mathbf{s}$. For identical separable Lipschitz continuous (LC) denoiser, $\eta_t(\mathbf{g}) = [\eta_t(g_1) \ \eta_t(g_2) \ \dots \ \eta_t(g_N)]^T$, and $\text{div}(\eta_t(\mathbf{g})) = \frac{1}{N} \sum_{j=1}^N \partial \eta_t(g_j) / \partial g_j$. Similarly, for non-separable LC denoisers, we have [13]

$$\eta_t(\mathbf{g}) = [\eta_{t,1}(g_1) \ \eta_{t,2}(g_2) \ \dots \ \eta_{t,L}(g_L)]^T, \quad (6)$$

and

$$\text{div}(\eta_t(\mathbf{g})) = \frac{1}{N} \sum_{m=1}^L \text{Tr}\left(\frac{\partial \eta_{t,m}(\mathbf{g}_m)}{\partial \mathbf{g}_m}\right), \quad (7)$$

where $\mathbf{g}_1, \mathbf{g}_2, \dots, \mathbf{g}_L$ denote L non-overlapping partitions of \mathbf{g} . The initial work on AMP focused on the case where $\eta_t(\cdot)$ is a separable elementwise function with identical components [12], while the later work allowed non-separable denoiser [13].

¹The corresponding probability mass function (PMF) of the PDF in (3) is $P\{\mathbf{x}_q = \sqrt{P_1} \mathbf{e}_k\} = \frac{1}{2^K}$, $k = 1, 2, \dots, 2^K$. Since for the problem at hand, we have both continuous and discrete random variables, Dirac's delta function is used to link discrete PMF to PDF.

For large, i.i.d., sub-Gaussian random matrices \mathbf{A} in (4)², $\lim_{M,N \rightarrow \infty} M/N \triangleq \beta > 0$, and identical separable/non-separable LC denoiser, AMP displays decoupling behavior, meaning that \mathbf{v}^t in (5c) behaves like an AWGN corrupted version of the true signal \mathbf{u} in (4) as [14]

$$\mathbf{v}^t = \mathbf{u} + \mathcal{N}(0, \sigma_t^2 \mathbf{I}), \quad (8)$$

where an estimate of σ_t^2 can be obtained as $\hat{\sigma}_t^2 = \frac{1}{M} \|\mathbf{r}^t\|^2$. The larger M , the lower the estimation error.

B. SE of AMP With Separable Denoiser

For large, i.i.d., sub-Gaussian random matrices \mathbf{A} , the performance of the AMP can be exactly predicted by a scalar SE, which also provides testable conditions for optimality. For identical separable LC denoiser $\eta_t(\cdot)$, when the elements of $\mathbf{u} = [u_1, u_2, \dots, u_N]^T$ empirically converges to some random variable U with probability density function (PDF) f_U , the SE, i.e., the sequence of $\{\sigma_t^2\}_{t \geq 0}$ in (8) is expressed as [15]

$$\sigma_{t+1}^2 = \sigma_w^2 + \frac{1}{\beta} \mathbb{E}\{(\eta_t(U + \sigma_t Z) - U)^2\}, \quad (9a)$$

$$\sigma_0^2 = \sigma_w^2 + \frac{1}{\beta} \mathbb{E}\{U^2\}, \quad (9b)$$

where $\beta \triangleq M/N$, $Z \sim \mathcal{N}(0, 1)$, and is independent from $U \sim f_U$. The term $(\sigma_{t+1}^2 - \sigma_w^2)\beta$ in (9a) can be estimated by the sample mean estimate of the denoiser error as [15]

$$\begin{aligned} \lim_{N \rightarrow \infty} \frac{1}{N} \|\hat{\mathbf{u}}^{t+1} - \mathbf{u}\|_2^2 &= \mathbb{E}\{(\eta_t(U + \sigma_t Z) - U)^2\} \\ &= (\sigma_{t+1}^2 - \sigma_w^2)\beta, \end{aligned} \quad (10)$$

where $\hat{\mathbf{u}}^{t+1} \triangleq [\hat{u}_1^{t+1} \ \hat{u}_2^{t+1} \ \dots \ \hat{u}_N^{t+1}]^T$ is obtained by using the AMP algorithm in (5a)-(5c).

IV. RBS-AMP MUD ALGORITHM

In this section, the separable MMSE denoiser for the approximate joint prior distribution of the sparse vector \mathbf{x} is obtained and then is used for Bayesian AMP soft decoding. This results in RBS-AMP MUD algorithm. The MUE of the proposed RBS-AMP MUD algorithm is also derived.

A. RBS-AMP MUD Algorithm With Separate Denoiser

The RBS-AMP MUD algorithm neglects the block-sparsity of \mathbf{x} in (1) and considers an i.i.d. distribution for its elements. Let $\eta(\mathbf{x}_q) \triangleq \prod_{k=1}^{2^K} f_X(x_{q,k}; P_1; K)$ denote an approximation of the joint prior distribution $\gamma(\mathbf{x}_q) \triangleq f_{\mathbf{X}}(\mathbf{x}_q; P_1, K)$ in (3). By minimizing the KLD between the corresponding PMFs of γ and η , we obtain

$$f_X(x; P_1; K) = \frac{1}{2^K} \delta(x - \sqrt{P_1}) + \left(1 - \frac{1}{2^K}\right) \delta(x). \quad (11)$$

This block sparsity relaxation results in a low complexity MUD algorithm because (3) is replaced with the simple joint prior distribution $\eta(\mathbf{x}_q)$. While $\eta(\mathbf{x}_q)$ allows the sparsity level of \mathbf{x}_q to be larger than one, the separable MMSE denoiser can correctly decode the one-hot vector because sparsity level one still has the highest prior probability.

Let $\hat{\mathbf{x}} = [\hat{x}_1^{t+1}, \hat{x}_2^{t+1}, \dots, \hat{x}_N^{t+1}]^T$ denote the reconstructed vector by the AMP algorithm summarized in (5a)-(5c) at the $(t+1)$ th iteration for the observation model in (1), i.e., $\mathbf{s} = \mathbf{y}$, $\mathbf{u} = \mathbf{x}$, and $\mathbf{A} = \mathbf{C}$. For the identical separable MMSE denoiser $\eta(v_i^t) = \mathbb{E}\{\cdot | v_i^t\}$ with prior distribution

$$2E\{A_{ij}\} = 0, E\{A_{ij}^2\} = \frac{1}{M}, \text{ and } E\{A_{ij}^6\} = \frac{C}{M}, \text{ for some fixed } C > 0.$$

$U = X \sim f_X(x; P_1; K)$ in (11), by taking into account the decoupling behavior in (8), the i th element of the soft decoded vector at the $(t + 1)$ th iteration is given by

$$\begin{aligned}\hat{x}_i^{t+1} &= \eta(v_i^t) = \mathbb{E}\{X_i|X_i + \sigma_t Z = v_i^t\} \\ &= \frac{\sqrt{P_1} p T_i^t}{p T_i^t + 1 - p},\end{aligned}\quad (12)$$

where $Z \sim \mathcal{N}(0, 1)$, $T_i^t \triangleq \exp\{\frac{-P_1+2v_i^t\sqrt{P_1}}{2\sigma_t^2}\}$, and $p = 1/2^K$. Proof of the general case for the prior PDF in (3) is given in Appendix A. Moreover, the divergence term at the $(t + 1)$ th iteration of the RBS-AMP MUD in (5b) is obtained as

$$\begin{aligned}\text{div}(\boldsymbol{\eta}_t(\mathbf{v}^t)) &= \frac{1}{N} \sum_{i=1}^N \frac{\partial}{\partial v_i^t} \eta_t(v_i^t) \\ &= \frac{1}{N} \sum_{i=1}^N \frac{\partial}{\partial v_i^t} \mathbb{E}\{X_i|X_i + \sigma_t Z = v_i^t\} \\ &= \frac{p(1-p)P_1}{\sigma_t^2 N} \sum_{i=1}^N \frac{T_i^t}{(p T_i^t + 1 - p)^2}.\end{aligned}\quad (13)$$

B. MUE of the RBS-AMP MUD Algorithm

The degradation in bit error rate due to the presence of MA interference in AWGN channel can be measured by the multiuser asymptotic efficiency, which is defined as

$$\xi = \frac{\sigma_w^2}{\sigma_w^2 + I}, \quad (14)$$

where σ_w^2 is the variance of noise, and I is the interference after soft decoding.

Theorem 1: The MUE of the RBS-AMP MUD algorithm at the $(t + 1)$ th iteration is given by

$$\xi_{\text{RB}}^{t+1} = \frac{\sigma_w^2}{\sigma_w^2 + (\sigma_{t+1}^2 - \sigma_w^2)} = \frac{\sigma_w^2}{\sigma_{t+1}^2}, \quad (15)$$

where $\xi_{\text{RB}}^{t+1} \in [0, 1]$, and σ_{t+1}^2 is given in (9a)-(9b) for $U = X$ in (11) (Proof in Appendix B).

In practice, the SE, i.e., $\{\sigma_t^2\}_{t \geq 0}$ is tracked by the sample mean estimate $\hat{\sigma}_t^2 \approx \frac{1}{M} \|\mathbf{r}^t\|^2$, where \mathbf{r}^t is given in (5b) for $\mathbf{s} = \mathbf{y}$, $\mathbf{A} = \mathbf{C}$ and $\hat{\mathbf{u}} = \hat{\mathbf{x}}$. The SE can also be theoretically obtained by using (10). In this case, from (10) and (11), we obtain (16) at the bottom of the page.

V. BS-AMP MUD ALGORITHM

In this section, we first in Theorem 2 show that the per-iteration mean-squared error of the reconstructed vector through AMP with non-separable denoiser can be predicted using a state evolution (SE). Then, the non-separable denoiser for the exact joint prior distribution of the sparse vector \mathbf{x} in (3) is obtained and is used for Bayesian AMP soft decoding. This results in the BS-AMP MUD algorithm. Theorem 2 will

be later used for the derivation of the MUE of the proposed BS-AMP MUD algorithm.

A. SE of AMP With Non-Separable Denoiser

Let us consider a block structure for the vector \mathbf{u} in (4) as $\mathbf{u} = [\mathbf{u}_1^T, \mathbf{u}_2^T, \dots, \mathbf{u}_L^T]^T$, where \mathbf{u}_i and \mathbf{u}_j , $i \neq j$ are independent random vectors. We consider the following cases: 1) the joint PDF of $\mathbf{u}_i \triangleq [u_{i,1}, u_{i,2}, \dots, u_{i,\ell}]^T$ is $\mathbf{U} = [U_1 \ U_2 \ \dots \ U_\ell]^T \sim f_U$, and 2) the empirical joint PDF of \mathbf{u}_i converges weakly to f_U , where $\ell = N/L$. AMP with identical non-separable LC denoiser in (6) with $\tilde{\eta}_t(\cdot) : \mathbb{R}^\ell \rightarrow \mathbb{R}^\ell$ ($\eta_{t,m}(\cdot) = \tilde{\eta}_t(\cdot)$, $m = 1, 2, \dots, L$), reconstructs the vector \mathbf{u} from the observation model in (4) through the relations in (5a)-(5c). Also, the decoupling behavior occurs for the m th block as

$$\mathbf{v}_m^t = \mathbf{u}_m + \mathbf{z}_m^t, \quad m = 1, 2, \dots, L, \quad (17)$$

where

$$\mathbf{z}_m^t \sim N(0, \rho_m^2 \mathbf{I}). \quad (18)$$

The SE, i.e., the sequence of $\{\rho_m^2\}_{t \geq 0}$ in (18) is given by

$$\rho_{t+1}^2 = \sigma_w^2 + \frac{1}{\ell \beta} \mathbb{E}\{\|\tilde{\eta}_t(\mathbf{U} + \rho_t \mathbf{Z}) - \mathbf{U}\|^2\}, \quad (19a)$$

$$\rho_0^2 = \sigma_w^2 + \frac{1}{\ell \beta} \mathbb{E}\{\|\mathbf{U}\|^2\}, \quad (19b)$$

where $\mathbf{Z} = [Z_1 \ Z_2 \ \dots \ Z_\ell]^T \sim N(0, \mathbf{I})$ is independent of $\mathbf{U} = [U_1 \ U_2 \ \dots \ U_\ell]^T \sim P_U$. A modified version of Theorem 1 for identical non-separable LC denoiser is given as follows.

Theorem 2: Let $\mathbf{A} \in \mathbb{R}^{M \times N}$ be a matrix with i.i.d. entries $A_{ij} \sim \mathcal{N}(0, 1/M)$, and assume $M/N \rightarrow \beta > 0$. Consider a block sparse signal $\mathbf{u} = [\mathbf{u}_1^T \ \mathbf{u}_2^T \ \dots \ \mathbf{u}_L^T]^T$, where the joint distribution of each block of length ℓ is f_U (or the empirical joint PDF converges weakly to f_U) on \mathbb{R}^ℓ . Then, we have

$$\lim_{L \rightarrow \infty} \frac{1}{L} \sum_{u=1}^L \|\hat{\mathbf{u}}_u^{t+1} - \mathbf{u}_u\|^2 = \mathbb{E}\{\|\tilde{\eta}_t(\mathbf{U} + \rho_t \mathbf{Z}) - \mathbf{U}\|^2\}, \quad (20)$$

where $\hat{\mathbf{u}} = [\hat{\mathbf{u}}_1^T \ \hat{\mathbf{u}}_2^T \ \dots \ \hat{\mathbf{u}}_L^T]^T$ is obtained by using (5a)-(5c), $\mathbf{U} \sim f_U$, $\mathbf{Z} \sim N(0, \mathbf{I})$ is independent of \mathbf{U} , and ρ_t follows the SE in (19a) and (19b) (Proof in Appendix C).

B. BS-AMP MUD Algorithm With Non-Separable Denoiser

By considering the exact prior distribution of \mathbf{x} in (3), AMP with block non-separable denoiser can be employed to reconstruct the vector $\mathbf{x} = [\mathbf{x}_1^T, \mathbf{x}_2^T, \dots, \mathbf{x}_D^T]^T$ from the under-determined system of linear equations $\mathbf{y} = \mathbf{Cx} + \mathbf{w}$ in (1) by using the relations (5a)-(5c). For identical block non-separable MMSE denoiser $\tilde{\eta}(\mathbf{v}_u^t) = \mathbb{E}\{\cdot | \mathbf{v}_u^t\} : \mathbb{R}^{2^K} \rightarrow \mathbb{R}^{2^K}$, the reconstructed vector for the u th IoT device at the $(t + 1)$ th iteration is given as follows

$$\hat{\mathbf{x}}_u^{t+1} = \mathbb{E}\{\mathbf{X} | \mathbf{X} + \rho_t \mathbf{Z} = \mathbf{v}_u^t\}, \quad (21)$$

where $\mathbf{X} = [X_1, X_2, \dots, X_{2^K}]^T$ is a random vector with the joint PDF in (3) and $\mathbf{v}_u^t = \hat{\mathbf{x}}_u^t + \mathbf{C}^T \mathbf{r}^t = \mathbf{x}_u + \mathcal{N}(0, \rho_t^2 \mathbf{I})$ due to the decoupling affect as it was explained in (17) in (18).

$$\begin{aligned}\lim_{N \rightarrow \infty} \frac{1}{N} \|\hat{\mathbf{x}}^{t+1} - \mathbf{x}\|_2^2 &= \mathbb{E}\{(\eta_t(X + \sigma_t Z) - X)^2\} = \frac{1}{2^K \sqrt{2\pi\sigma_t^2}} \int_{-\infty}^{\infty} \left(\frac{\sqrt{P_1} p T_i^t}{p T_i^t + 1 - p} - \sqrt{P_1} \right)^2 \exp\left\{-\frac{(v_i^t - \sqrt{P_1})^2}{2\sigma_t^2}\right\} dv_i^t \\ &\quad + \left(1 - \frac{1}{2^K}\right) \frac{1}{\sqrt{2\pi\sigma_t^2}} \int_{-\infty}^{\infty} \left(\frac{\sqrt{P_1} p T_i^t}{p T_i^t + 1 - p} \right)^2 \exp\left\{-\frac{(v_i^t)^2}{2\sigma_t^2}\right\} dv_i^t = (\sigma_{t+1}^2 - \sigma_w^2)\beta.\end{aligned}\quad (16)$$

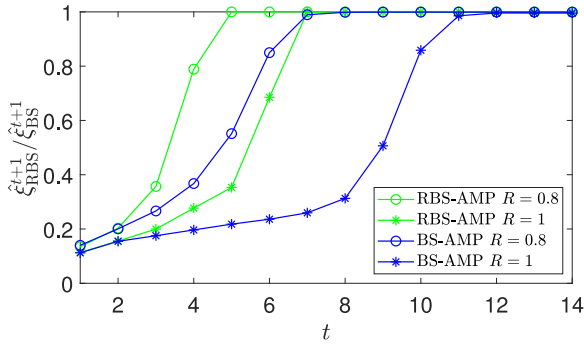


Fig. 1. State evolution of the RBS-AMP and BS-AMP MUD algorithms for $K = 8$ and $D = 256$ at $E_b/N_0 = 6$ dB.

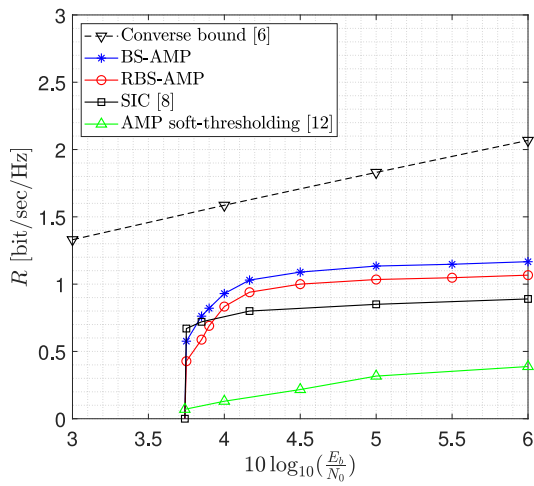


Fig. 2. Spectral efficiency versus $10 \log_{10}(E_b/N_0)$ for the average block error rate $P_e = 15 \times 10^{-4}$, $K = 8$, and $D = 256$.

By employing (3) and the fact that $\mathbf{Z} \sim \mathcal{N}(\mathbf{0}, \mathbf{I})$, $\hat{\mathbf{x}}_u^{t+1}$ in (21) is obtained as

$$\begin{aligned}\hat{\mathbf{x}}_u^{t+1} &= \tilde{\eta}(\mathbf{v}_u^t) = \mathbb{E}\{\mathbf{X}|\mathbf{X} + \rho_t \mathbf{Z} = \mathbf{v}_u^t\} \\ &= \frac{\sqrt{P_I} \sum_{k=1}^{2^K} \exp\left\{-\frac{\|\mathbf{v}_u^t - \sqrt{P_I} \mathbf{e}_k\|_2^2}{2\rho_t^2}\right\} \mathbf{e}_k}{\sum_{m=1}^{2^K} \exp\left\{-\frac{\|\mathbf{v}_u^t - \sqrt{P_I} \mathbf{e}_m\|_2^2}{2\rho_t^2}\right\}},\end{aligned}\quad (22)$$

where $\mathbf{e}_1, \mathbf{e}_2, \dots, \mathbf{e}_{2^K}$ are orthonormal basis (Proof in Appendix A).

By using (7) and (22) and after some simplifications, the divergence for the MMSE non-separable denoiser is derived as in (23), shown at the bottom of the page. The RBS-AMP MUD algorithm offers a lower complexity compared to the BS-AMP MUD algorithm due to the simple separable MMSE denoiser. On the other hand, the BS-AMP MUD algorithm achieves a higher spectral efficiency compared to the RBS-AMP MUD algorithm because of the non-separable MMSE denoiser that uses the exact joint PDF.

C. MUE of the BS-AMP MUD Algorithm

At the $(t+1)$ th iteration of the BS-AMP algorithm, we have $\hat{\mathbf{x}}^{t+1} \triangleq [\hat{\mathbf{x}}_1^{t+1} \ \hat{\mathbf{x}}_2^{t+1} \ \dots \ \hat{\mathbf{x}}_D^{t+1}]^T$, where $\hat{\mathbf{x}}_u^{t+1}$ is given (22). Similar to the RBS-AMP algorithm in Appendix B, we can obtain the MUE for the BS-AMP algorithm. For $D \rightarrow \infty$, by taking into account Theorem 2 for $L = D$ and $\ell = 2^K$, using the fact that $\mathbf{C}^T \mathbf{C} = \mathbf{I}$ ($N \rightarrow \infty$, $M \rightarrow \infty$), and employing (19a) and (20), we can write the interference term as $I^{t+1} = (\rho_{t+1}^2 - \sigma_w^2)$, where $\rho_{t+1}^2 = \sigma_w^2 + \frac{1}{2^K \beta} \mathbb{E}\{\|\tilde{\eta}(\mathbf{X} + \rho_t \mathbf{Z}) - \mathbf{X}\|^2\}$ and $\rho_0^2 = \sigma_w^2 + \frac{1}{2^K \beta} \mathbb{E}\{\|\mathbf{X}\|^2\}$. By substituting I^{t+1} into (14), we obtain the MUE of the BS-AMP MUD algorithm at the $(t+1)$ th iteration as follows

$$\xi_{BA}^{t+1} = \frac{\sigma_w^2}{\sigma_w^2 + (\rho_{t+1}^2 - \sigma_w^2)} = \frac{\sigma_w^2}{\rho_{t+1}^2}. \quad (24)$$

VI. SIMULATION RESULTS

In practice, the sample mean estimate of $\{\sigma_t^2\}_{t \geq 0}$ and $\{\rho_t^2\}_{t \geq 0}$, i.e., $\frac{1}{M} \|\mathbf{r}^t\|$ is employed to track the MUE of the RBS-AMP and the BS-AMP MUD algorithms as $\frac{M \sigma_w^2}{\|\mathbf{r}^{t+1}\|}$. In Fig. 1, we show the estimated MUE for $K = 8$ and $D = 256$ at $E_b/N_0 = 6$ dB. As seen, $\hat{\xi}_{RB}^{t+1} = 1$ and $\hat{\xi}_{BA}^{t+1} = 1$ are achieved. Also, the lower the spectral efficiency R the faster the decoding.

In Fig. 2, we show the spectral efficiency R [bits/sec/Hz] versus $10 \log_{10}(E_b/N_0)$ for average block error rate $P_e = 15 \times 10^{-4}$, $K = 8$, and $D = 256$. We also illustrate the spectral efficiency of the AMP with soft-thresholding [12], the SIC decoding in [8], and the upper bound in [6]. As expected, the BS-AMP outperforms the RBS-AMP since the non-separable MMSE denoiser in more efficiently suppresses noise. Moreover, as seen, both algorithms outperform the AMP with soft-thresholding and the SIC. For packets of 8 information bits, the BS-AMP and RBS-AMP MUD algorithms reach $4/7$ and $1/2$ of the upper bound at $E_b/N_0 = 4$ dB, respectively.

VII. CONCLUSION

Two new MUD algorithms for massive G-MAC with short-packet transmission were developed in this letter. Our proposed MUD algorithms were developed based on AMP with non-separable and separable MMSE denoisers. Our results show that the proposed MUD algorithms offer superior soft decoding performance compared to the state-of-the-art AMP with soft-threshold denoising. This higher spectral efficiency is achieved with low computational complexity for massive G-MAC with short-packet transmission due to decoupling effect.

APPENDIX A

For the proposed BS-AMP MUD with block non-separable MMSE denoiser with the prior PDF in (3), we have

$$\hat{\mathbf{x}}_u^{t+1} = \mathbb{E}\{\mathbf{X}|\mathbf{X} + \rho_t \mathbf{Z} = \mathbf{v}_u^t\} = \int_{\mathcal{R}^{2^K}} \mathbf{x}_u f_{\mathbf{X}|\mathbf{V}}(\mathbf{x}_u | \mathbf{v}_u^t; K) d\mathbf{x}_u$$

$$\begin{aligned}\text{div}(\eta_t(\mathbf{v}^t)) &= \frac{1}{N} \sum_{u=1}^D \text{Tr} \frac{\partial \tilde{\eta}_t(\mathbf{v}_u^t)}{\partial \mathbf{v}_u^t} = \frac{\sqrt{P_I}}{N} \sum_{u=1}^D \frac{1}{\sum_{n=1}^{2^K} \exp\left\{-\frac{\|\mathbf{v}_u^t - \sqrt{P_I} \mathbf{e}_n\|_2^2}{2\rho_t^2}\right\}} \sum_{k=1}^{2^K} \frac{(\sqrt{P_I} - v_{u,k})}{\rho_t^2} \exp\left\{-\frac{\|\mathbf{v}_u^t - \sqrt{P_I} \mathbf{e}_k\|_2^2}{2\rho_t^2}\right\} \\ &- \frac{\sqrt{P_I}}{N} \sum_{u=1}^D \frac{1}{\left[\sum_{n=1}^{2^K} \exp\left\{-\frac{\|\mathbf{v}_u^t - \sqrt{P_I} \mathbf{e}_n\|_2^2}{2\rho_t^2}\right\}\right]^2} \sum_{k=1}^{2^K} \exp\left\{-\frac{\|\mathbf{v}_u^t - \sqrt{P_I} \mathbf{e}_k\|_2^2}{2\rho_t^2}\right\} \sum_{m=1}^{2^K} \frac{(\sqrt{P_I} \delta[k-m] - v_{u,k})}{\rho_t^2} \exp\left\{-\frac{\|\mathbf{v}_u^t - \sqrt{P_I} \mathbf{e}_m\|_2^2}{2\rho_t^2}\right\}.\end{aligned}\quad (23)$$

$$\begin{aligned}
&= \int_{\mathcal{R}^{2K}} \mathbf{x}_u \frac{f_{\mathbf{V}|\mathbf{X}}(\mathbf{v}_u^t | \mathbf{x}_u; K) f_{\mathbf{X}}(\mathbf{x}_u; P_I, K)}{\int_{\mathcal{R}^{2K}} f_{\mathbf{V}|\mathbf{X}}(\mathbf{v}_u^t | \mathbf{z}; K) f_{\mathbf{X}}(\mathbf{z}; P_I, K) d\mathbf{z}} d\mathbf{x}_u \\
&= \sqrt{P_I} \sum_{k=1}^{2^K} \frac{f_{\mathbf{V}|\mathbf{X}}(\mathbf{v}_u^t | \bar{\mathbf{e}}_k; K)}{\sum_{m=1}^{2^K} f_{\mathbf{V}|\mathbf{X}}(\mathbf{v}_u^t | \bar{\mathbf{e}}_m; K)} \mathbf{e}_k,
\end{aligned} \tag{25}$$

where $f_{\mathbf{V}|\mathbf{X}}(\mathbf{v}_u^t | \mathbf{x}; K)$ ($f_{\mathbf{X}|\mathbf{V}}(\mathbf{x} | \mathbf{v}_u^t; K)$) denotes the conditional PDF of the random vector \mathbf{v}_u^t (\mathbf{x}) given random vector \mathbf{x} (\mathbf{v}_u^t), and $\bar{\mathbf{e}}_k \triangleq \sqrt{P_I} \mathbf{e}_k$. The last equality in (25) is obtained by replacing (3) in the third equality and then using $\int_{\mathcal{R}^{2K}} \delta(\mathbf{x} - \mathbf{x}_0) d\mathbf{x} = 1$. Moreover, due to the decoupling effect, we can write $\mathbf{v}_u^t = \mathbf{x}_u + \mathcal{N}(0, \rho_t^2 \mathbf{I})$; thus, we have

$$f_{\mathbf{V}|\mathbf{X}}(\mathbf{v}_u^t | \mathbf{x}_u; K) = \frac{1}{\eta} \exp \left\{ \frac{-\|\mathbf{v}_u^t - \mathbf{x}_u\|^2}{2\rho_t^2} \right\}, \tag{26}$$

where $\eta \triangleq (2\pi\rho_t^2)^{2^{K-1}}$. Finally, by substituting (26) into (25), we obtain (22). Similarly, for the RBS-AMP MUD algorithm, we can write

$$\begin{aligned}
\hat{x}_i^{t+1} &= \eta(v_i^t) = \mathbb{E}\{X_i | X_i + \sigma_t Z = v_i^t\} \\
&= \int_{-\infty}^{+\infty} x_i f_{X|V}(x_i | v_i^t; K) dx_i \\
&= \frac{p\sqrt{P_I} f_{V|X}(v_i^t | x_i = \sqrt{P_I}; K)}{p f_{V|X}(v_i^t | x_i = \sqrt{P_I}; K) + (1-p) f_{V|X}(v_i^t | x_i = 0; K)},
\end{aligned} \tag{27}$$

where $p = 1/2^K$. By substituting $f_{V|X}(v_i^t | x_i; K) = \frac{1}{\sqrt{2\pi}} \exp\{-(v_i^t - x_i)^2 / 2\sigma_t^2\}$ into (27), and after some simplification, we obtain (12).

APPENDIX B

At the $(t+1)$ th iteration of the RBS-AMP algorithm, we have $\hat{\mathbf{x}}^{t+1} \triangleq [\hat{x}_1^{t+1} \ \hat{x}_2^{t+1} \ \dots \ \hat{x}_N^{t+1}]^\top$, where x_i^{t+1} is given in (12). By employing (1) and the fact that \mathbf{w} is independent of \mathbf{x} and \mathbf{v}_u^t (due to decoupling), the average reconstruction error \mathcal{E} at the $(t+1)$ th iteration of the RBS-AMP algorithm can be written as

$$\begin{aligned}
\mathcal{E}^{t+1} &= \frac{1}{M} \mathbb{E}\{(\mathbf{y} - \mathbf{C}\hat{\mathbf{x}}^{t+1})^\top (\mathbf{y} - \mathbf{C}\hat{\mathbf{x}}^{t+1})\} \\
&= \frac{1}{M} \mathbb{E}\{\mathbf{w}^\top \mathbf{w}\} + \frac{1}{M} \mathbb{E}\{(\mathbf{x} - \hat{\mathbf{x}}^{t+1})^\top \mathbf{C}^\top \mathbf{C}(\mathbf{x} - \hat{\mathbf{x}}^{t+1})\}.
\end{aligned} \tag{28}$$

The first term in (28) denotes the noise power σ_w^2 , and the second term is the interference at the $(t+1)$ th iteration, i.e., I^{t+1} . By using (10), for $N \rightarrow \infty$, we can write

$$\begin{aligned}
\frac{1}{N} \mathbb{E}\{(\mathbf{x} - \hat{\mathbf{x}}^{t+1})^\top (\mathbf{x} - \hat{\mathbf{x}}^{t+1})\} &= \frac{1}{N} (\mathbf{x} - \hat{\mathbf{x}}^{t+1})^\top (\mathbf{x} - \hat{\mathbf{x}}^{t+1}) \\
&= \mathbb{E}\{(\eta(X + \sigma_t Z) - X)^2\} = (\sigma_{t+1}^2 - \sigma_w^2)\beta,
\end{aligned} \tag{29}$$

where $\beta = M/N$ and σ_{t+1}^2 is given in (9a) by replacing U with X . Moreover, for $N \rightarrow \infty$ and $M \rightarrow \infty$, we have $\mathbf{C}^\top \mathbf{C} = \mathbf{I}$. Considering this equality and (29), we can write

$$\begin{aligned}
I^{t+1} &= \frac{1}{M} \mathbb{E}\{(\mathbf{x} - \hat{\mathbf{x}}^{t+1})^\top \mathbf{C}^\top \mathbf{C}(\mathbf{x} - \hat{\mathbf{x}}^{t+1})\} \\
&= \frac{1}{M} (\mathbf{x} - \hat{\mathbf{x}}^{t+1})^\top (\mathbf{x} - \hat{\mathbf{x}}^{t+1}) = (\sigma_{t+1}^2 - \sigma_w^2).
\end{aligned} \tag{30}$$

By substituting (30) into (14), we obtain the MUE of the RBS-AMP MUD algorithm at the $(t+1)$ th iteration as in (15).

APPENDIX C

For the proof, we need to show that the sample mean estimator in (20) is consistent [16]. Let us define random variable

$Q_t \triangleq \|\tilde{\mathbf{y}}_t(\mathbf{U} + \rho_t \mathbf{Z}) - \mathbf{U}\|^2$ with finite mean $\theta_t \triangleq \mathbb{E}\{Q_t\}$. The sample mean estimate of θ_t is given by $\hat{\theta}_{t,L} = \frac{1}{L} \sum_{l=1}^L q_{t,l} = \frac{1}{L} \sum_{u=1}^L \|\hat{\mathbf{u}}_u^{t+1} - \mathbf{u}_u\|^2$, where $q_{t,l}$, $l = 1, 2, \dots, L$, are i.i.d. drawn from random variable Q_t , and the second inequality comes from the decoupling behavior in (17) and (18) and the denoising operation in (5a). By using Markov's inequality, we can write

$$P(|\hat{\theta}_{t,L} - \theta_t| > \epsilon_t) \leq \frac{\mathbb{E}\{|\hat{\theta}_{t,L} - \theta_t|\}}{\epsilon_t}. \tag{31}$$

For the sample mean estimator $\hat{\theta}_{t,L}$, we have

$$|\hat{\theta}_{t,L} - \theta_t|^2 = \left| \frac{1}{L} \sum_{l=1}^L q_{t,l} - \theta_t \right|^2 \leq \frac{1}{L^2} \sum_{l=1}^L |q_{t,l} - \theta_t|^2. \tag{32}$$

By applying the statistical expectation to both sides of (32), and then using (31), we obtain [4]

$$P(|\hat{\theta}_{t,L} - \theta_t|^2 > \epsilon_t^2) \leq \frac{\sigma_{Q_t}^2}{L\epsilon_t^2}, \tag{33}$$

where $\mathbb{E}\{(Q_t - \theta_t)^2\} = \sigma_{Q_t}^2 = \mathbb{E}\{|q_{t,l} - \theta_t|^2\}$. The right-hand side of (33) goes to zero as $L \rightarrow \infty$. Hence, for any small positive values ϵ_t , we can write

$$\lim_{L \rightarrow \infty} P\left(\left| \frac{1}{L} \sum_{u=1}^L \|\hat{\mathbf{u}}_u^{t+1} - \mathbf{u}_u\|^2 - \theta_t \right|^2 \geq \epsilon_t^2\right) = 0. \tag{34}$$

REFERENCES

- [1] M. Mohammadkarimi, M. A. Raza, and O. A. Dobre, "Signature-based nonorthogonal massive multiple access for future wireless networks: Uplink massive connectivity for machine-type communications," *IEEE Veh. Technol. Mag.*, vol. 13, no. 4, pp. 40–50, Dec. 2018.
- [2] M. Mohammadkarimi, O. A. Dobre, and M. Z. Win, "Massive uncoordinated multiple access for beyond 5G," *IEEE Trans. Wireless Commun.*, vol. 21, no. 5, pp. 2969–2986, May 2022.
- [3] U. K. S. Shiv, S. Bhashyam, C. R. Srivatsa, and C. R. Murthy, "Learning-based sparse recovery for joint activity detection and channel estimation in massive random access systems," *IEEE Wireless Commun. Lett.*, vol. 11, no. 11, pp. 2295–2299, Nov. 2022.
- [4] L. Liu, E. G. Larsson, W. Yu, P. Popovski, C. Stefanovic, and E. De Carvalho, "Sparse signal processing for grant-free massive connectivity: A future paradigm for random access protocols in the Internet of Things," *IEEE Signal Process. Mag.*, vol. 35, no. 5, pp. 88–99, Sep. 2018.
- [5] R. B. Di Renna, C. Bockelmann, R. C. de Lamare, and A. Dekorsy, "Detection techniques for massive machine-type communications: Challenges and solutions," *IEEE Access*, vol. 8, pp. 180928–180954, 2020.
- [6] I. Zadik, Y. Polyanskiy, and C. Thrampoulidis, "Improved bounds on Gaussian MAC and sparse regression via Gaussian inequalities," in *Proc. ISIT*, 2019, pp. 430–434.
- [7] J. Choi, "NOMA-based compressive random access using Gaussian spreading," *IEEE Trans. Commun.*, vol. 67, no. 7, pp. 5167–5177, Jul. 2019.
- [8] R. R. Müller, "Massive Gaussian multiple-access by random coding with soft interference cancellation," in *Proc. IEEE ICC*, 2021, pp. 1–6.
- [9] M. Mayer and N. Goertz, "Bayesian optimal approximate message passing to recover structured sparse signals," 2015, *arXiv:1508.01104*.
- [10] A. Ma, Y. Zhou, C. Rush, D. Baron, and D. Needell, "An approximate message passing framework for side information," *IEEE Trans. Signal Process.*, vol. 67, no. 7, pp. 1875–1888, Apr. 2019.
- [11] S. Rangan, "Generalized approximate message passing for estimation with random linear mixing," in *Proc. ISIT*, 2011, pp. 2168–2172.
- [12] D. L. Donoho, A. Maleki, and A. Montanari, "Message-passing algorithms for compressed sensing," *Proc. Nat. Acad. Sci. USA*, vol. 106, no. 45, pp. 18914–18919, 2009.
- [13] R. Berthier, A. Montanari, and P.-M. Nguyen, "State evolution for approximate message passing with non-separable functions," *Inf. Inference J. IMA*, vol. 9, no. 1, pp. 33–79, Jan. 2019.
- [14] C. Rush and R. Venkataraman, "Finite sample analysis of approximate message passing algorithms," *IEEE Trans. Inf. Theory*, vol. 64, no. 11, pp. 7264–7286, Nov. 2018.
- [15] M. Bayati and A. Montanari, "The dynamics of message passing on dense graphs, with applications to compressed sensing," *IEEE Trans. Inf. Theory*, vol. 57, no. 2, pp. 764–785, Feb. 2011.
- [16] M. G. Kendall and A. Stuart, *The Advanced Theory of Statistics*. London, U.K.: Griffin, 1961.